

## True three-dimensional image reconstruction by nuclear magnetic resonance zeugmatography

C-M Lai†§ and P C Lauterbur†‡

Departments of Chemistry† and Radiology‡, State University of New York at Stony Brook, Stony Brook, NY 11794, USA

Received 12 December 1979, in final form 29 April 1980

**Abstract.** Nuclear magnetic resonance (NMR) zeugmatographic imaging may become a safe and versatile alternative to medical imaging techniques that employ ionising and ultrasonic radiation. Most of the techniques that have been described for obtaining NMR images use single point, line, or plane scans to give a single slice, or reconstruct only a two-dimensional projection, and are relatively inefficient, complex, or difficult to scale up for use on the human body. There are a number of advantages to scanning simultaneously an approximately spherical volume to obtain a true three-dimensional image. A simple two-stage reconstruction method is described for obtaining such images efficiently with isotropic resolution, and examples are presented to demonstrate the validity and usefulness of this mode. The feasibility of high-resolution imaging on large objects is also discussed.

### 1. Introduction

Although three-dimensional nuclear magnetic resonance (NMR) imaging was proposed long ago (Lauterbur 1973), very few examples of this technique for obtaining such images have been described (Lauterbur *et al* 1977, Lauterbur and Lai 1980). True three-dimensional imaging has a number of advantages over the sequential imaging of points, lines and planes, and over two-dimensional reconstruction. No review of these alternative methods will be given here, but references and discussions may be found in the papers by Hinshaw (1976), Mansfield and Maudsley (1976), Andrew *et al* (1977), Brooker and Hinshaw (1978), and Lauterbur (1979a, b).

Because the resolution that can be achieved in NMR zeugmatographic imaging will often be limited by the signal-to-noise ratio obtainable from a volume element during the total scan time (Hoult and Lauterbur 1979, Lauterbur 1979b), the efficient use of all of the nuclear magnetisation within an object is essential if the optimal resolution, contrast and imaging time are to be realised. If the spins in the entire volume of an object, or that portion of it lying within the radiofrequency transmitting and receiving coils, are excited, the NMR signal in a magnetic field gradient will be a one-dimensional projection of all of the signals from the three-dimensional region. The reconstruction of a three-dimensional image from such projections uses all of the signal from the active volume, and may give an image with isotropic resolution, so that all slices or views are equivalent. Such true 3D images are, therefore, quite different from those assembled from sequentially-scanned slices, whose thickness is usually much greater than the resolution in the plane of the slice. Both the efficiency and the quality of true 3D images

§ Present address: Analogic Corporation, Audubon Road, Wakefield, MA 01880, USA.

are better, in principle, than those for tomographic images. Nuclear magnetic resonance techniques are ideally suited to generating such images.

## **2. Method and experimental results**

True three-dimensional nuclear magnetic resonance images can be reconstructed by a two-stage filter back-projection algorithm. The mathematical analysis of the reconstruction technique has been presented previously (Lai and Lauterbur 1980). In a typical experiment, the zero-dimensional signal, obtained as the impulse response from the entire object in a homogeneous magnetic field, is converted to a one-dimensional representation of the spatial distribution of the NMR signals by the imposition of a magnetic field gradient. If the gradient is linear, each such representation corresponds to a projection resulting from integration of the signal over planes perpendicular to the gradient direction. Rotation of the gradient direction in a plane perpendicular to any axis generates a set of one-dimensional projections from which a two-dimensional image, as seen from a direction along that axis, may be reconstructed. Rotation of the gradient about another axis generates data from which another such image may be reconstructed. Any desired two-dimensional views may be obtained, without any mechanical motion of the object or the scanning apparatus, because linear magnetic field gradients combine vectorially, so that any desired gradient direction may be produced by appropriate adjustment of the currents in three sets of coils.

From a set of two-dimensional views, or projections, a three-dimensional image may be obtained by a second stage of reconstruction, as shown in figure 1. Only three two-dimensional reconstructed projections are shown, for simplicity and clarity. Each has its normal lying in the  $YX$  plane, and from each, a strip of signal intensity may be chosen at a particular value of  $z$  and used to reconstruct a slice of the three-dimensional object. This procedure may be repeated to generate a complete three-dimensional array, which may be displayed as slice images with any orientation. As an example of

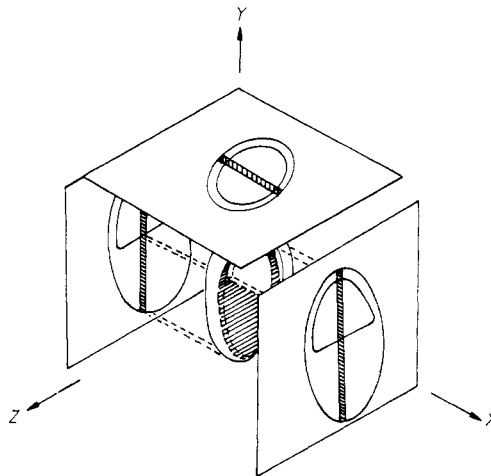


**Figure 1.** Representative views used in a two-stage three-dimensional reconstruction. Each two-dimensional projection has been reconstructed from a number of one-dimensional projections (such as that shown for a real object in figure 3). A reconstructed slice of the three-dimensional image is shown. The coordinate axes are those used in the experiments.

the use of this technique, we have reconstructed a complete three-dimensional image of a coconut from 30 two-dimensional pictures, each of which was reconstructed from 30 one-dimensional projections. The object was contained within the 4 MHz radio-frequency transmitter-receiver coil, as shown in figure 2, and in a magnetic field of

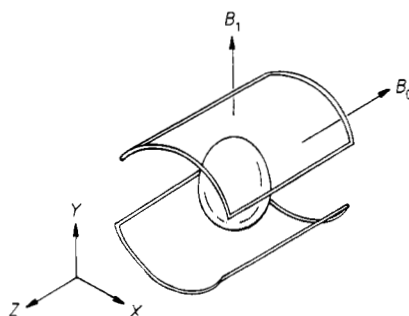


**Figure 2.** The location of an object within a schematic set of radiofrequency transmitting-receiving coils. The directions of  $B_0$ , the static magnetic field, and  $B_1$ , the radiofrequency magnetic field, are shown. The  $B_1$  field is stronger near the wires, causing the slight brightening observed in those regions in figure 5.

93.8 mT. Linear gradients of approximately  $500 \mu\text{T m}^{-1}$  were used. Each one-dimensional projection was obtained by Fourier transformation of a single free induction decay following a  $45^\circ$  radiofrequency pulse (Lauterbur and Lai 1980). A typical projection is shown in figure 3, and two sets of 16 two-dimensional images, each

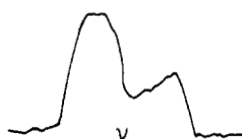


**Figure 3.** A one-dimensional projection of a coconut, obtained as the Fourier transform of a single 4 MHz free induction decay following a radiofrequency pulse. Phase adjustments and base-line corrections have been made.

reconstructed on a  $33 \times 33$  array, are shown in figure 4, with the whole set displayed as a  $256 \times 256$  array. From all 30 such images, the complete three-dimensional array was reconstructed. It is displayed in figure 5 as 16 vertical slices, each 5 mm in thickness. The resolution in the plane of each slice is also approximately 5 mm, and is limited by the small number of views taken. The entire data acquisition time for the 900 projections required 12 min, and was limited by the slow transfer of data from core memory to magnetic tape in the computer system used. Because each 2D image was reconstructed from 30 projections distributed over 360 degrees at  $12^\circ$  intervals, the resolution was the equivalent of that obtainable with 15 projections. The opposing projections were averaged to minimise certain experimental artifacts, especially those arising because of small phase shifts in the detected signals. Similarly, the 30 2D projections were distributed over 360 degrees, imposing an additional two-fold redundancy. The 3D resolution, therefore, is the equivalent of that obtainable with 225 projections, and the signal-to-noise ratio has been increased by approximately a factor of two by the overall four-fold redundancy.

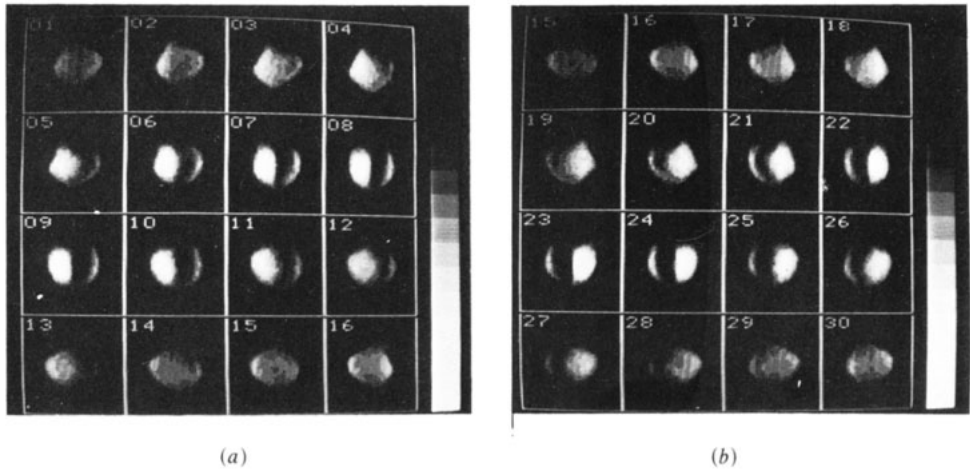


**Figure 4.** (a) The first 16 two-dimensional projected images of the coconut, each reconstructed from 30 one-dimensional projections such as that shown in figure 3. (b) The last 16 two-dimensional images (Nos 15 and 16 are duplicates of those in (a)). Note that, because a full 360° rotation was used, the second half of these projections should be mirror images of the first half.

Another example is shown in figure 6. A preserved pig heart, its interior filled with air, was imaged under the conditions described above, but with slightly greater resolution because of its smaller size, since the size of the reconstruction array can be adjusted to the size of the object being imaged. The empty chambers of the heart are clearly resolved, as well as the major vessels at its base. A portion of the heart wall, visible in the original images at low intensity, does not appear in these reproductions. Had the chambers been filled with blood, the contrast would have been much lower, since only proton concentrations are being measured in these experiments. Additional

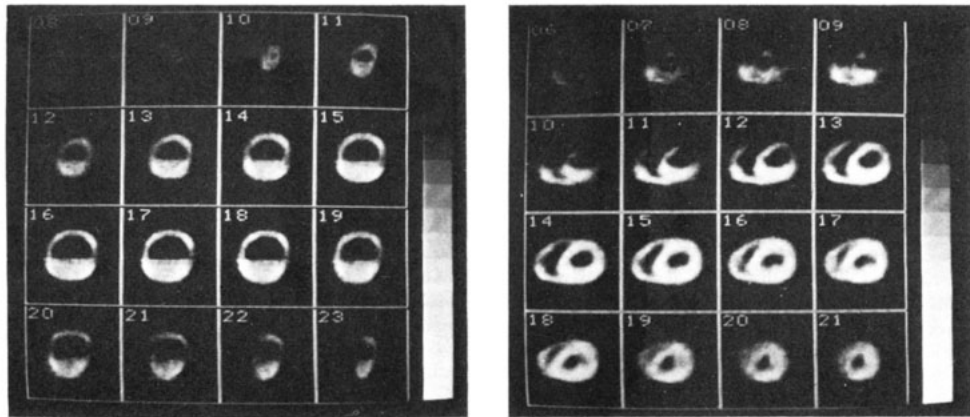


**Figure 5.** The reconstructed true three-dimensional image of the coconut, displayed as a set of plane slices perpendicular to the Z direction. The outer slices fade because there is appreciable  $B_1$  and  $B_0$  inhomogeneity in those regions.

**Figure 6.** A reconstructed true three-dimensional image of a preserved pig heart, displayed as a set of plane slices perpendicular to the Z direction. The heart was empty. A portion of the thin wall is not visible in these reproductions, but can be seen on the original video display.

contrast can be generated by making use of relaxation time differences (Lauterbur 1973).

### 3. Discussion and conclusions

True three-dimensional NMR imaging by reconstruction from one-dimensional projections, which represent integrals over planes of constant magnetic field, is more efficient in the use of the limited NMR signal intensities and gives well-resolved images even with a small number of projections, such as the 225 independent projections used to obtain the images shown above. It should be noted that a  $33 \times 33 \times 33$  array (35,937 voxels) was reconstructed from data acquired in 12 min, so that the effective scanning time per slice at this resolution was only about 22 s. If the projections were not redundant, the data acquisition of 225 projections would be reduced to 3 min. Furthermore, the scan time in this experiment was mainly limited by a slow data storage system to a sampling rate of 800 ms per projection. In a test that collected data but did not store the data for processing, the sampling rate was increased to 100 ms per projection without reducing the signal intensities noticeably. Under this optimisation, the total data acquisition time to resolve an NMR image on a  $128 \times 128 \times 128$  array, which requires 3600 independent projections with each projection consisting of 128 data points, would be 6 min. For comparison, the data acquisition speed of a recent x-ray CT scanner is about 20 ms per projection.

The computation time for a large 3D array reconstruction is realistic as well. To reconstruct from 3600 projections on a  $128 \times 128 \times 128$  array, there will be 60 reconstructions in the first stage, and another 128 reconstructions in the second stage, on a two-dimensional  $128 \times 128$  array. A commercial hardware reconstructor, such as Analogic XAP-400, can reconstruct an image of  $128 \times 128$  array from 60 projection angles in about 160 ms. If such a hardware reconstructor were used, the total reconstruction time, excluding the input/output time and the data management time, would take only 30 s for the  $128 \times 128 \times 128$  array. With this machine, it would be possible to process the first-stage reconstructions in real time. Although none of the 128 slice images would be obtained during the scan, they could be reconstructed in the second stage one by one right after the completion of the scan.

In this experiment, the NMR signals were detected by a single-phase detector, and the phase errors were automatically corrected by a software program (Lai and Lauterbur 1981). If a dual-phase detection system were implemented, the sensitivity could be improved by a factor of approximately two. A more powerful magnet could also be built. If the magnetic field strength were doubled, the signal-to-noise ratio would increase about four fold. The transmitter-receiver coil and the radio frequency preamplifier were not optimised in sensitivity either. Taking all these factors into consideration, it seems possible to improve the performance considerably, and to obtain practical NMR zeugmatographic images of the human body with three-dimensional resolution better than the slice thickness usually used in x-ray CT scanning, and perhaps approaching the resolution of CT images in the scanning plane.

### Acknowledgments

This investigation was partly supported by Grant No CA-153000, awarded by the National Cancer Institute, DHEW, and by Grant No HL1985101A1, awarded by the National Heart, Lung and Blood Institute, DHEW.

## Résumé

Reconstruction d'images tri-dimensionnelle vraie en zeugmatographie par résonance magnétique nucléaire.

L'imagerie par zeugmatographie par résonance magnétique nucléaire (RMN) peut devenir une alternative viable et ayant de larges applications aux techniques d'imagerie médicale employant des rayonnements ionisants ou des ultra-sons. La plupart des techniques qui ont été décrites utilisent des balayages d'un seul point, d'une ligne ou d'un plan pour donner une coupe unique ou pour reconstruire seulement une projection bi-dimensionnelle, et sont relativement inefficaces, complexes ou difficiles à étalonner pour l'utilisation sur le corps humain. Il existe un certain nombre d'avantages à balayer simultanément un volume approximativement sphérique pour obtenir une image réellement tri-dimensionnelle. On décrit une méthode simple de reconstruction en deux stades pour obtenir efficacement de telles images avec une résolution isotrope et nous présentons des exemples pour montrer la validité et l'utilité de cette méthode. Nous discutons également la possibilité d'obtenir des images de haute résolution sur de grands objets.

## Zusammenfassung

Echte dreidimensionale Bildkonstruktion mit der Kernspinresonanz-Zeugmatographie.

Die zeugmatografische Bildverarbeitung wird eine sichere und vielseitige Alternative zu medizinischen Bildverarbeitungstechniken, die ionisierende Strahlung und Ultraschall verwenden. Die meisten Techniken, die zur Erhaltung von NMR-Bildern beschrieben worden sind, benutzen Einzelpunkt-, Linien- oder ebene Scans für eine einzelne Schicht, oder rekonstruieren nur eine zweidimensionale Projektion und sind relativ ineffizient, komplex oder schwierig zu vergrößern für den menschlichen Körper. Es gibt einige Vorteile beim simultanen Scanning eines näherungsweise sphärischen Volumens um ein echtes dreidimensionales Bild zu erhalten. Beschrieben wird eine einfache Zwei-Stufen Rekonstruktionsmethode, um solche Bilder mit isotroper Auflösung zu erhalten. Es werden Beispiele präsentiert, die die Gültigkeit und Nützlichkeit der Methode demonstrieren. Die Anwendung hochauflösender Bildgebungsverfahren bei großen Objekten wird diskutiert.

## References

- Andrew E R, Bottomley P A, Hinshaw W S, Holland G N, Moore W S, and Simaraj C 1977 *Phys. Med. Biol.* **22** 971-4
- Brooker H R and Hinshaw W S 1978 *J. Magn. Resonance* **30** 129-31
- Hinshaw W S 1976 *J. Appl. Phys.* **47** 3709-21
- Hoult D I and Lauterbur P C 1979 *J. Magn. Resonance* **34** 425-33
- Lai C-M and Lauterbur P C 1980 *J. Phys. E: Sci. Instrum.* **13** 747-50
- Lai C-M and Lauterbur P C 1981 *J. Phys. E: Sci. Instrum.* **14** 874-80
- Lauterbur P C 1973 *Nature* **242** 190-1
- Lauterbur P C, Chen C-N and Lai C-M 1977 paper presented at the 6th Int. Symp. on Magnetic Resonance, Banff, Canada
- Lauterbur P C 1979a *IEEE Trans. Nucl. Sci.* **NS-26** 2808-11
- Lauterbur P C 1979b in *Medical Imaging Techniques*, eds K Preston, K J W Taylor, S A Johnson and W R Ayers (New York: Plenum Press) 209-18
- Lauterbur P C and Lai C-M 1980 *IEEE Trans. Nucl. Sci.* **NS-27** 1227-31
- Mansfield P and Maudsley A A 1976 *Phys. Med. Biol.* **21** 847-52